Journal of Photochemistry & Photobiology, A: Chemistry 434 (2023) 114228

Contents lists available at ScienceDirect

Journal of Photochemistry & Photobiology, A: Chemistry

journal homepage: www.elsevier.com/locate/jphotochem

Evaluation of the anticancer activity and chemiluminescence of a halogenated coelenterazine analog

José Pedro Silva [a], Patricia González-Berdullas [a], Mariana Pereira [b,c], Diana Duarte [b,c], José E. Rodríguez-Borges [d], Nuno Vale [b,c,e], Joaquim C.G. Esteves da Silva [a,f], Luís Pinto da Silva [a,f,*]

[a] Chemistry Research Unit (CIQUP), Institute of Molecular Sciences (IMS), Department of Geosciences, Environment and Territorial Planning, Faculty of Sciences, University of Porto), Rua do Campo Alegre s/n, 4169-007 Porto, Portugal
[b] OncoPharma Research Group, Center for Health Technology and Services Research (CINTESIS), Rua Doutor Plácido da Costa, 4200-450 Porto, Portugal
[c] CINTESIS@RISE, Faculty of Medicine, University of Porto, Al. Prof. Hernàni Monteiro, 4200, 319 Porto, Portugal
[d] LAQV/REQUIMTE, Department of Chemistry and Biochemistry, Faculty of Sciences, University of Porto, Rua do Campo Alegre s/n, 4169-007 Porto, Portugal
[e] Department of Community Medicine, Health Information and Decision (MEDCIDS), Faculty of Medicine, University of Porto, Rua Doutor Plácido da Costa, 4200-450 Porto, Portugal
[f] LACOMEPHI, GreenUPorto, Department of Geosciences, Environment and Territorial Planning, Faculty of Sciences, University of Porto), Rua do Campo Alegre s/n, 4169-007 Porto, Portugal

ARTICLE INFO

Keywords:
Chemiluminescence
Coelenterazine
Cancer Therapy
Superoxide Anion
Sensing
Drug Combination

ABSTRACT

Chemiluminescence is a remarkable process in which light is emitted due to a chemical reaction, without the need for photoexcitation. Among some of the most well-known chemiluminescent systems is that of marine Coelenterazine. Herein, we report the synthesis of a novel halogenated Coelenterazine analog, as well as the characterization of its potential anticancer activity and chemiluminescence. We have found that this analog is capable of significantly enhanced emission in aqueous solution when triggered by superoxide anion while being compatible with human cell lines. So, this compound presents great potential for the sensitive and dynamic sensing of a molecule of interest in biological media. Furthermore, the analysis of its cytotoxicity provided structural insight into the properties of brominated Coelenterazines, which were previously found to possess selective anticancer activity. Namely, the introduction of bromine heteroatoms is not enough to provide cytotoxicity, while the introduction of electro-withdrawing groups eliminates all previously reported anticancer activity. Finally, while this compound is not active, its use in a combination approach allowed to improve the profile of a known chemotherapeutic agent. These results should be useful to guide future optimizations of halogenated Coelenterazine analogs.

1. Introduction

Bioluminescence and chemiluminescence are processes in which thermal energy is converted into excitation energy, leading to the emission of light [1–3]. While different chemi- and bioluminescent systems have their specificities, in general light is emitted as the result of the same two-step process [4–6]. Namely, the reactions typically start with the oxygenation of the reactant, leading to the formation and subsequent thermolysis of energy-rich peroxide intermediates. These thermolysis pathways allow for the thermally-activated singlet ground state (S_0) to be chemiexcited directly into the first singlet excited state (S_1) of the light-emitter, which subsequently decays to the S_0 state by emission of visible light.

While a great number of different chemi- and bioluminescent systems exist [2,7], Coelenterazine (Chart 1) is one of the most well-known chemi- and bioluminescent substrates [2,7–9]. More specifically, ~80% of all bioluminescent organisms are found in the oceans, and most of them use Coelenterazine and other imidazopyrazinone-based natural derivatives (as *Cypridina* and *Watasenia* luciferins, Chart 1) as bioluminescent substrates [10]. Interestingly, Coelenterazine is capable both of chemiluminescence (in aprotic solvents or in the presence of superoxide anion) [11–16], and bioluminescence (in presence of luciferase enzymes

* Corresponding author.
E-mail address: luis.silva@fc.up.pt (L. Pinto da Silva).

https://doi.org/10.1016/j.jphotochem.2022.114228
Received 11 June 2022; Received in revised form 16 August 2022; Accepted 20 August 2022
Available online 24 August 2022

or photoproteins) [17–20].

One of the most important features of all chemi- and bioluminescent processes (including that of Coelenterazine and derivatives) is that they are associated with a diminished probability of autofluorescence arising from the background signal (increasing the signal-to-noise ratio), as they do not require photoexcitation [7,8]. Given this, the chemi-/bioluminescent signal can be generated with high sensitivity and almost no background noise [7,8]. This feature is quite important for different applications in biological media, leading to the increasing use of chemi- and bioluminescent systems in sensing [12,15,21–26] and real-time bioimaging [27–30].

For Coelenterazine, specifically, one of the most recent applications based on its lack of photoexcitation is its use as the basis for tumor-selective and self-activating photosensitizers for photodynamic therapy (PDT) of cancer. PDT is a minimally-invasive anticancer therapy with few side effects and a fast healing rate of healthy tissues [31,32]. More specifically, it consists in the administration of a photosensitizer that accumulates in tumor tissue. After that, the tumor site is irradiated with light of specific wavelengths, which photoexcites the photosensitizer from its S_0 state to its S_1 one, from which it undergoes intersystem crossing (ISC) to triplet states (T_1). The T_1 photosensitizer is now able to interact with molecular oxygen, leading to the formation of the highly cytotoxic singlet oxygen by energy transfer [31–33]. The advantageous features of PDT make it an anticancer therapy with significant potential. However, its dependence on external light sources limits it to superficial tumors, due to the low penetration depth of light into biological tissues [34,35]. This dependence also means that PDT is unable to treat metastatic tumors [35].

Thus, optimization of PDT requires the development of novel tumor-selective photosensitizers capable of intracellular self-activation without an external light source. In recent years, members of this team have been using the chemiluminescent reaction of Coelenterazine as a basis for such sensitizers [36–39]. More specifically, one of the chemiluminescent reactions of Coelenterazine is triggered solely by superoxide anion (without any catalyst/co-factor) [36–39], which is typically overexpressed in tumor cells [25]. Furthermore, the chemiluminescent reactions of Coelenterazines and other imidazopyrazinones also present a pathway for $S_0 \rightarrow T_1$ ISC [40], despite being considered inefficient given that this system is known for the effective generation of singlet excited states [2,7]. Thus, if the efficiency of this ISC step is enhanced, Coelenterazine could directly generate T_1 states capable of sensitizing singlet oxygen inside the cell in response to a tumor marker [36–39].

One of the most common strategies to enhance ISC is the introduction of heavy atoms such as bromine [33]. Given this, members of this team have been focused on developing Coelenterazine derivatives that possess bromine heteroatoms at different positions besides presenting different functionalization degrees [36–39]. Rather interestingly, different derivatives showed superoxide anion-triggered singlet oxygen sensitization and presented relevant anticancer activity toward both prostate and breast cancer, while not inducing toxicity toward non-cancer cells [36,37]. Thus, these compounds show potential as prototypical photosensitizers capable of tumor-selective self-activation without the need for external light sources, thereby addressing the disadvantages of PDT.

One of these Coelenterazine brominated analogs (Cla) was OHBr-Cla (Chart 2), which maintained the imidazopyrazinone core and the phenol moiety (where the hydroxyl group acted as an electron donor group, EDG) while substituting the benzyl and *p*-cresol moieties by a bromine heteroatom (a halogen, heavy-atom, and electron-withdrawing group, EWG) and a methyl group, respectively [36]. Another somewhat similar Cla compound was Br-Cla (Chart 2), in which the hydroxyl (EDG) group of the phenol was substituted by a bromine heteroatom (a halogen, heavy-atom, and EWG), while the *p*-cresol and benzyl moieties were replaced by a methyl group and a hydrogen atom, respectively [37,38]. Both compounds presented activity toward both prostate and cancer cells (IC_{50} values present in Chart 2), albeit with different magnitudes. The anticancer activity of OHBr-Cla was not relevant for breast cancer while being significantly more effective for prostate cancer (Chart 2) [36]. As for Br-Cla, its activity was very similar for both cancer types (Chart 2) [37,38].

Herein, our objective is to investigate if we can optimize the anticancer activity of these Cla compounds, as well as to determine how sensitive their activity is regarding minor structural modifications. To this end, we have designed and synthesized the novel FBr-Cla (Chart 2), which was created as a hybrid of both OHBr-Cla and Br-Cla. As in both compounds, the *p*-cresol of Coelenterazine is replaced by a methyl group (Chart 2). As in OHBr-Cla (Chart 2), the benzyl moiety of Coelenterazine is replaced by a bromine heteroatom (a halogen, heavy-atom, and EWG) to enhance the $S_0 \rightarrow T_1$ ISC pathway during chemiluminescence [37,38]. It should be noted that Br-Cla also possesses a bromine heteroatom for that purpose but in another position (Chart 2) [37,38]. Finally, as in Br-Cla (Chart 2), the hydroxyl group of the phenol is replaced by a halogen and EWG. However, to better evaluate the sensitivity of the compounds to minor modifications, that halogen is not the heavier bromine, but instead the lighter fluorine. By adding this heteroatom to that position, it will also help to assess how changing that group from an EDG to EWG affects the anticancer activity of OHBr-Cla-like compounds, while not being masked by the addition of further heavy-atom effects (which would occur if instead of fluorine, we added a second bromine heteroatom).

FBr-Cla was subjected to an in-depth luminometric and photophysical characterization of its superoxide anion-induced chemiluminescent reaction. Its anticancer activity toward breast and prostate cancer cell lines (to compare with both Br-Cla and OHBr-Cla) was evaluated *in vitro* for the first time, while its safety toward non-cancer cells was also determined. This approach will then allow us to obtain further structural insight into the properties of brominated Cla compounds, to guide the development of much-needed self-activating and tumor-selective photosensitizers for light-free PDT.

2. Materials and methods

2.1. Synthesis of FBr-Cla

The complete description of the synthetic procedure for FBr-Cla can be found in the Supporting Information. In short, the first step is a

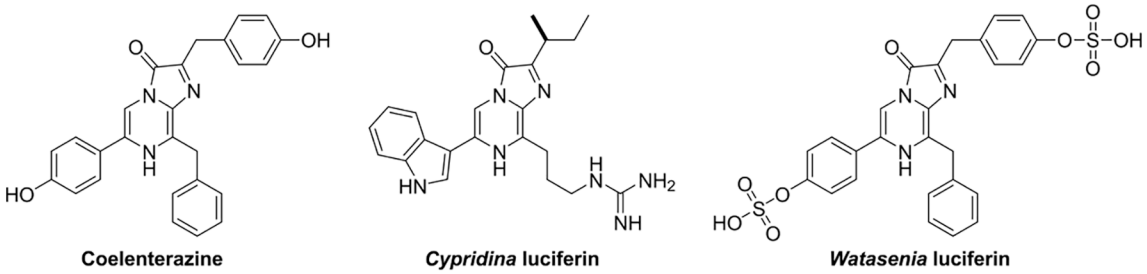

Chart 1. Molecular structures of Coelenterazine, *Cypridina* luciferin, and *Watasenia* luciferin.

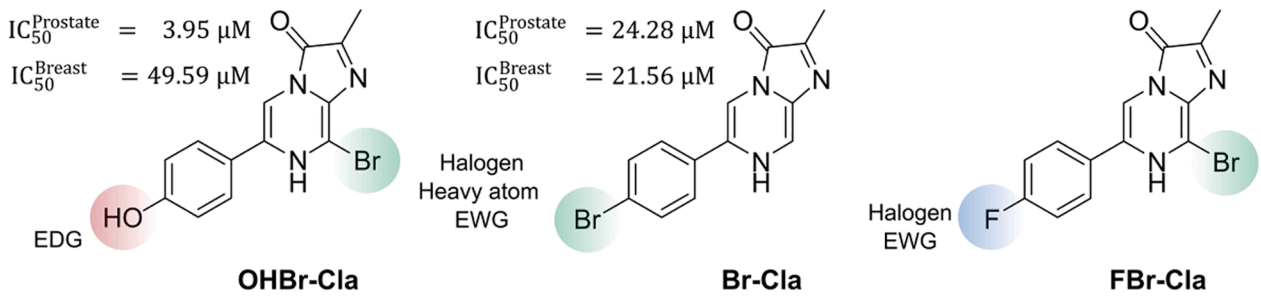

Chart 2. Molecular structures of OHBr-Cla, Br-Cla, and FBr-Cla. EWG refers to electron-withdrawing groups, while EDG refers to electron donor groups. IC_{50} values (in μM) were obtained toward prostate and breast cancer cell lines in [36,37].

Suzuki-Miyaura cross-coupling between 4-fluorophenylboronic acid and commercial 5-bromopyrazin-2-amine in THF, to yield 5-(4-fluorophenyl)pyrazin-2-amine (F-Clm). A bromine heteroatom was added to F-Clm by addition of *N*-bromosuccinimide in ethanol, which resulted in 3-bromo-5-(4-fluorophenyl)pyrazine-2-amine (FBr-Clm). Finally, methylglyoxal was added (in acid media) to form the imidazopyrazinone core through a cyclization reaction, leading to FBr-Cla. The structural characterization of F-Clm, FBr-Clm, and FBr-Cla was performed by ^{1}H and ^{13}C NMR spectroscopy (**Figures S1-S3**) and FT-MS spectrometry (**Figures S4-S6**).

2.2. Luminometric and photophysical investigations

Chemiluminescence kinetic studies were performed in a homemade luminometer using a Hamamatsu HC135-01 photomultiplier tube (Hamamatsu, Japan). All reactions took place at room temperature at least in sextuplicate, with light being integrated and recorded in 0.1 s intervals. The UV–vis spectra of FBr-Cla were also obtained at room temperature in a VWR® UV–vis spectrophotometer (UV-3100PC, VWR, United State) with a quartz cuvette. Fluorescence spectra were measured with a Horiba Jovin Fluoromax 4 spectrofluorometer (Horiba, Japan) with an integration time of 0.1 s. Slit widths of 5 nm were used for both the excitation and emission monochromators. Chemiluminescence spectra were obtained with the same spectrofluorometer, but with slit width of 29 nm for the emission monochromator. Quartz cuvettes were also used for the fluorescence and chemiluminescence spectra.

2.3. Cell, media, and compounds

MRC-5 lung fibroblast, MCF-7 human mammary carcinoma, and PC-3 human prostate carcinoma cell lines were obtained from the American Type Culture Collection (ATCC; Manassas, VA, USA), and were grown in a humidified incubator with 5% CO_2 at 37 °C in DMEM medium supplemented with 10% fetal bovine serum (FBS) and 1% penicillin–streptomycin (pen-strep) solution. These reagents were purchased on Millipore Sigma (Merck KGaA, Darmstadt, Germany). The medium was changed every 96 h.

2.4. Cell viability assay

Cell viability was measured using the MTT (Thiazolyl blue tetrazolium bromine; cat. No. M5655; Sigma-Aldrich; Merck KGaA, Darmstadt, Germany) assay in 96-well plates. For the protocol, 8,000 (MCR-5), 10,000 (MCF-7), and 5,000 (PC-3) cells in 200 μL of medium were grown per well for 24 h at 37 °C. Then, cells were treated with FBr-Cla in the following concentrations: 1, 25, 50, and 100 μM. Control cells were treated with 0.1% methanol (vehicle). The cell viability of the combination of increasing FBr-Cla (1, 25, 50, and 100 μM) with the IC_{50} of 5-Fluoroacil (5-FU, 11.79 μM) in PC-3 and MCF-7 cells was also measured. The controls were treated with 0.1% methanol and 0.1% DMSO (vehicles).

After incubation for 48 h at 37 °C, cell media were aspirated and 100 μL of MTT solution (0.5 mg/mL in PBS) was added to each well. After incubation for 3 h at 37 °C protected from light, MTT solution was removed from each well and 100 μL of DMSO were added to each well to solubilize the formazan crystals. Absorbance was measured on a Tecan Infinite M200 plate reader (Tecan Group ltd., Mannedorf, Switzerland) at 570 nm. Cell viability was calculated relative to the absorbance of carrier controls. Average values were obtained by performing three independent cell viability assays (n = 3).

2.5. Morphological analysis

Changes in cell morphology were evaluated after cell treatment using a Leica DMI 6000B microscope equipped with a Leica DFC350 FX camera (Leica Microsystems, Wetzlar, Germany). Images were analyzed with the Leica LAS X imaging software (v3.7.4) (Leica Microsystems, Wetzlar, Germany).

2.6. Statistical analysis

Cell viability graphs were obtained using the software GraphPad Prism 9 (GraphPad Software Inc., San Diego, CA, USA) after conducting three independent experiments (n = 3). Results are represented as the mean ± SEM for n experiments performed. Statistical analysis was performed with one-way ANOVA tests by Dunnett's multiple comparisons between control and treatment groups. Results were considered statistically significant for p values < 0.05.

3. Results and discussion

3.1. Chemistry and photophysical characterization of FBr-Cla

The proposed Cla compound was obtained by an initial Suzuki-Miyaura cross-coupling reaction between 4-fluorophenylboronic acid and commercial 5-bromopyrazin-2-amine. The resulting intermediate was halogenated to introduce a bromine heteroatom in *ortho* to the amine group, which was followed by a cyclization step with addition of methylglyoxal to yield FBr-Cla. This procedure was already validated and optimized by members of this team for obtaining several Cla compounds [12,36–38]. The structures of FBr-Cla and the synthesis intermediates were confirmed with both $^{1}H/^{13}C$ NMR and FT-MS spectroscopy (**Figures S1-S6**).

The absorption spectrum of FBr-Cla in aqueous solution is presented in Fig. 1. This spectrum is composed of sharp and more intense absorption bands in the ~200–230 nm range. Two more peaks can be found at ~260 and ~350 nm, while a shoulder at ~ 400 nm is also observed. In Fig. 1 is also presented the 2D excitation-emission matrix (EEM) contour plot for FBr-Cla, also in aqueous solution. This compound presents two emissive centers, but with the same fluorescence wavelength maximum (~425 nm). The two centers result from two different excitation bands, with maxima at ~270 and ~340 nm, which overlap

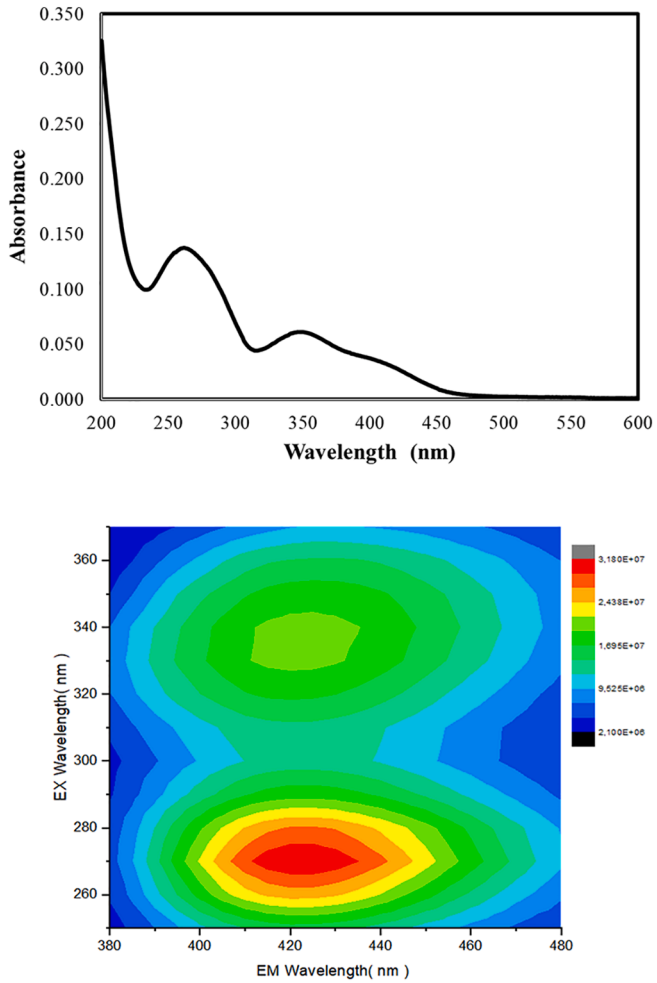

Fig. 1. UV–vis spectrum (top) and 2D excitation-emission (EEM) contour plot (bottom) for FBr-Cla (30 μM) in aqueous solution.

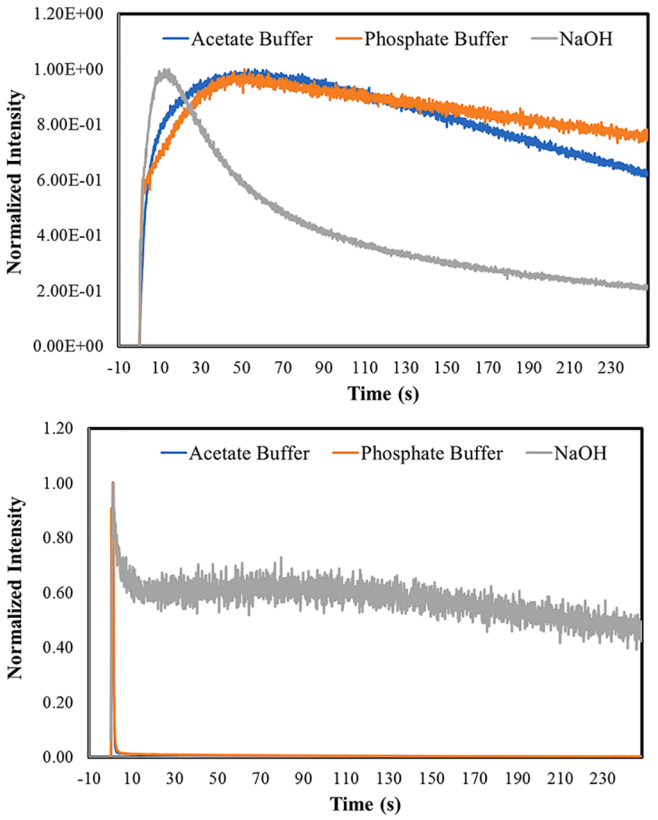

Fig. 2. Normalized chemiluminescence kinetic profile (top) for FBr-Cla in DMF with addition of either sodium acetate buffer pH 5.2 (1%), phosphate buffer pH 7.4 (75 mM), or NaOH (0.1 M). Normalized chemiluminescence kinetic profile (bottom) for FBr-Cla in aqueous solution with addition of either sodium acetate buffer pH 5.2 (1%), phosphate buffer pH 7.4 (75 mM), or NaOH (0.1), in the presence of 10 mg of potassium superoxide. All assays depicted here were performed for a final volume of 500 μL and a concentration of either 10 (in DMF) or 5 μM (in aqueous solution) for FBr-Cla.

with the absorption bands present in the UV–vis spectrum of this compound. Thus, the different emissive centers should result only from excitation to different excited states, which are converted into the same lowest singlet excited state (as stated by Kasha's rule). The photophysical properties found here are quite similar to those of another Cla previously synthesized by us (the main difference is that the emission of FBr-Cla is ~25 nm blue-shifted), which is similar to FBr-Cla, with the only difference being replacing the fluorine heteroatom with a methoxy group [12].

3.2. Luminometric investigation into the chemiluminescence of FBr-Cla

The first step of the luminometric investigation was to measure the chemiluminescence kinetic profile of FBr-Cla in the aprotic solvent *N*,*N*-dimethylformamide (DMF), in which Coelenterazine and derivatives are known to readily generate chemiluminescence by reacting with dissolved oxygen [13,41,42]. These measurements were performed in acidic, neutral, and basic pH, in conditions usually utilized in studies regarding chemiluminescence [12,13,36–38,41–44]. More specifically, measurements in basic pH were performed by the addition of NaOH (0.1 M), in neutral pH by adding phosphate buffer pH 7.4 (75 mM), and in acidic pH by adding sodium acetate buffer pH 5.2 (1%).

The chemiluminescence kinetic profiles (light-emission as a function of time), while normalized, are shown for different pH values in Fig. 2. We can see that the addition of DMF to FBr-Cla induces a very quick initial burst of light, which reaches maximum values under a minute. Thus, the new derivative is still chemiluminescent, despite its structural modifications. Interestingly, while the profiles found at acidic and neutral pH are almost identical, they show relevant differences from the profile obtained at basic pH. Namely, at basic pH, the profile is a somewhat typical flash profile, with a quick decay after reaching the light-emission maximum. However, at lower pH, the decay is relevantly lower. Thus, the chemiluminescence of FBr-Cla appears to be pH-sensitive.

A quantitative evaluation of the chemiluminescence output was made by measuring the light-emission intensity maxima (in relative

Table 1
Light-emission intensity maxima (in RLU), area of emitted light (in RLU), initial velocities (in RLU/s), and half-life (in s) for the chemiluminescence reactions of FBr-Cla in DMF with the addition of either sodium acetate buffer pH 5.2 (1%), phosphate buffer pH 7.4 (75 mM), or NaOH (0.1 M). Assays were performed for a final volume of 500 μL and a FBr-Cla concentration of 10 μM. Typical integration times for measurements were 0.1 s.

Solvent	Emission Intensity (RLU)	Emission Area (RLU)	Initial Velocities (RLU/s)	Half-life (s)
DMF + acetate buffer	$1.05 \times 10^4 \pm 8.42 \times 10^2$	$2.18 \times 10^6 \pm 1.75 \times 10^5$	$3.33 \times 10^3 \pm 3.12 \times 10^2$	344[a] ± 26
DMF + phosphate buffer	$1.09 \times 10^4 \pm 1.15 \times 10^3$	$1.93 \times 10^6 \pm 1.34 \times 10^5$	$1.27 \times 10^4 \pm 4.21 \times 10^3$	562[a] ± 63
DMF + NaOH	$1.45 \times 10^4 \pm 6.37 \times 10^2$	$1.59 \times 10^6 \pm 3.81 \times 10^4$	$1.50 \times 10^4 \pm 2.47 \times 10^3$	73.1 ± 4.7

[a]Integration times of 1 s.

light units, RLUs) and calculated area of light emission (in RLU), which are presented in Table 1 [11–14]. The initial velocities (RLU/s) and half-lives (s) of chemiluminescence emission were also determined (Table 1). Initial velocities are obtained by the increase in light production over the first milliseconds after the start of the reaction in the linear range of the chemiluminescence profile [12,45,46].

There are no great variations in magnitude in the light-emission maxima as a function of pH. Nevertheless, there is a relative increase in the maximum intensity with increasing pH, which is interesting as it has the opposite effect to what is typically observed for Coelenterazine and derivatives [11,42,44]. However, FBr-Cla still follows the typical behaviour of this type of compound in terms of initial velocities, as this parameter increases with increasing pH [11,42,44]. Interestingly, the half-life of chemiluminescence emission for these compounds is also somewhat pH-sensitive, since this parameter is relevantly higher at acidic-neutral pH (344–562 s) than at basic pH (73.1 s). Nevertheless, the higher half-life is found at neutral pH, meaning that pH is not the sole determining factor regarding the chemiluminescence half-life of FBr-Cla. It should be noted that while typical measurements were obtained with integration times of 0.1 s, the longer half-life at lower pH made it necessary to obtain this parameter with higher integration times (1 s). Longer half-life values should be useful for analytical/imaging purposes, as they should facilitate the detection of the analytical signal. Interestingly, the calculated areas of light emission decrease somewhat with increasing pH, which is contrary to the results of emission intensity (Table 1). Given this, and the behaviour of initial velocities, we can conclude that the kinetics of the CL reaction at basic pH are quicker, which result in a faster and more intense initial burst of light but does not result in a higher light output [12]. The behaviour of calculated area as a function of pH is more in line with was found previously for Coelenterazine and derivatives [11,12,42,44], and could be related with the chemical equilibria of the dioxetanone intermediate. That is, there is some evidence that neutral dioxetanone (which could be expected to be found at neutral pH) leads to more efficient chemiexcitation than its anionic counterpart (which could be expected to be found at basic pH) [11,13,41].

The chemiluminescence spectra of FBr-Cla was measured in DMF with addition of either sodium acetate buffer pH 5.2 (1%) or NaOH (0.1 M), which can be found in Fig. 3. The spectra consist of a single band at both pH conditions, with emission at basic pH being slightly blue-shifted (~440 nm) than at acidic pH (~460 nm). Another relevant difference between spectra is that the band at acidic pH is somewhat broad and less well-defined, to the contrary of the band found at basic pH (which is well-defined). One potential explanation for these pH-induced differences is that there could be two emitters, one at each pH condition, which is not strange for imidazopyrazinone-based molecules and is related with the chemical equilibria of the amide group of the Coelenteramide light-emitter [8,12,13]. In fact, a similar analog to FBr-Cla, in which fluorine is replaced by a methoxy group [12], showed dual emission at acidic pH (~410 and ~ 460 nm), while only a single band was found at basic pH (~460 nm).

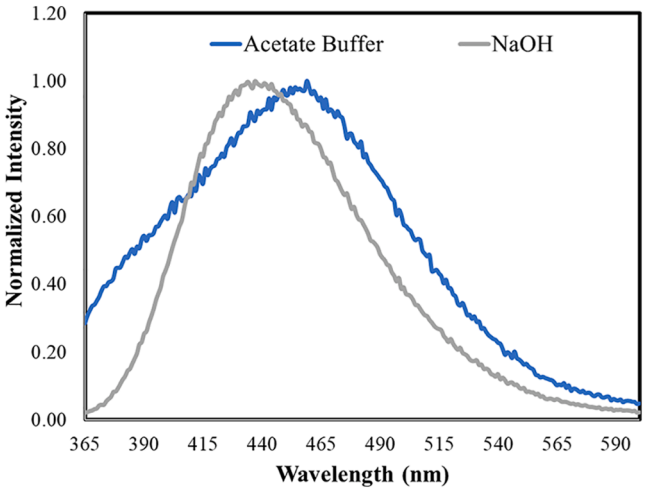

Fig. 3. Normalized chemiluminescence spectra for FBr-Cla in DMF with addition of either sodium acetate buffer pH 5.2 (1%), or NaOH (0.1 M).

The next step of this study was then to assess if superoxide anion can trigger the chemiluminescent reaction of FBr-Cla in aqueous solution. To perform this evaluation, the chemiluminescence kinetic profile of FBr-Cla was obtained in the presence of increasing amounts of potassium superoxide. This latter molecule is a typical source of superoxide anion in protic solvents, having already been used with success in the study of Cla compounds [12,37,38]. These measurements were made at different pH ranges, by addition of sodium acetate buffer pH 5.2 (1%), phosphate buffer pH 7.4 (75 mM), and NaOH (0.1 M). The normalized and representative chemiluminescent kinetic profiles at different conditions (in the presence of 10 mg of superoxide anion) are presented in Fig. 2.

It should be noted that the kinetic profiles found in the presence of superoxide anion and in aprotic solvents (Fig. 2) can be quite different, as chemiluminescence tends to decay quicker in the former conditions. This can be attributed to the known instability of superoxide anion in aqueous solution, which is explained by strong solvation and spontaneous disproportionation [47,48]. Interestingly, the kinetic profiles in aqueous solution at acidic and neutral pH are almost identical, with a clear and sharp flash profile. This is not the case at basic pH, in which the light-emission maximum is achieved rather quickly, but the light decay is slower and almost shaped like a plateau.

A quantitative evaluation of the chemiluminescent reactions monitored in aqueous solution was performed by measuring the light-emission intensity maxima (in RLU), calculated area of light emission (in RLU) and initial velocities (in RLU/s), which are presented in Table 2. In these conditions, the light-emission decay is too quick to allow for the proper determination of half-life values [12]. The results indicate a relevant and similar pH-sensitivity for both parameters. More specifically, the light-emission is significantly more intense with decreasing pH (both in terms of emission intensities and areas), while also being more efficient (according to the initial velocities). These results point to the chemiluminescent reaction, by itself, of FBr-Cla being more efficient at acidic pH. While the calculated area varied with pH in a similar manner in both aqueous solution and DMF, the emission intensities did not. This means that while part of this behaviour is related with intrinsic features of this chemiluminescent reaction, there are aspects that should be specific to superoxide anion-induced chemiluminescence in aqueous solution. For example, part of the enhancing effect of pH in aqueous solution could be directly related with the interaction between FBr-Cla and superoxide anion. Namely, it is expected that at more basic pH the imidazopyrazinone core becomes negatively charged, by the deprotonation of the NH group (Chart 1 and Chart 2) [37]. This could impair its interaction with the also negatively charged superoxide anion. In fact, this is what we observe in Fig. 2 and Table 2, with the reaction being less efficient and slower.

Interestingly, the chemiluminescence of FBr-Cla is sensitive to the amount of superoxide anion at all considered pH ranges (Table 2). Namely, increasing amounts of superoxide anion leads to the decrease of both the light-emission maxima intensity and initial velocities, at all pH ranges. Given that this is observed at different pH values, this feature should be an intrinsic characteristic of the system, and not dependent on different ionization states. Furthermore, as superoxide anion is a mild oxidant, these results indicate that FBr-Cla might be sensitive to over-oxidation by superoxide anion. Nevertheless, these results show that the chemiluminescence of FBr-Cla can be triggered (in a dose-dependent manner) by a general cancer marker (superoxide anion) [25].

To better assess the effect of our structural modifications on the intrinsic ability of imidazopyrazinones to be triggered by superoxide anion, we have also compared the chemiluminescence of FBr-Cla with

Table 2
Light-emission intensity maxima (in RLU), area of emitted light (in RLU) and initial velocities (in RLU/s) for the chemiluminescence reactions of FBr-Cla in aqueous solution with the addition of either sodium acetate buffer pH 5.2 (1%), phosphate buffer pH 7.4 (75 mM), or NaOH (0.1 M). Assays were performed for a final volume of 500 μL and a FBr-Cla concentration of 5 μM, as well as different amounts of potassium superoxide (5–15 mg).

Acetate Buffer			
Potassium superoxide (mg)	Emission Intensity (RLU)	Emission Area (RLU)	Initial Velocities (RLU/s)
5	$5.82 \times 10^5 \pm 2.79 \times 10^4$	$1.37 \times 10^6 \pm 1.68 \times 10^5$	$1.05 \times 10^6 \pm 9.92 \times 10^4$
10	$3.72 \times 10^5 \pm 2.80 \times 10^4$	$3.64 \times 10^6 \pm 2.66 \times 10^6$	$1.16 \times 10^6 \pm 1.21 \times 10^5$
15	$4.14 \times 10^5 \pm 3.17 \times 10^4$	$4.78 \times 10^5 \pm 2.18 \times 10^4$	$9.87 \times 10^5 \pm 1.06 \times 10^5$
Phosphate Buffer			
Potassium superoxide (mg)	Emission Intensity (RLU)	Emission Area (RLU)	Initial Velocities (RLU/s)
5	$3.17 \times 10^5 \pm 1.49 \times 10^4$	$1.01 \times 10^6 \pm 1.07 \times 10^5$	$6.85 \times 10^5 \pm 1.45 \times 10^5$
10	$2.09 \times 10^5 \pm 1.60 \times 10^4$	$1.70 \times 10^5 \pm 2.87 \times 10^4$	$6.05 \times 10^5 \pm 1.12 \times 10^5$
15	$7.38 \times 10^4 \pm 8.52 \times 10^3$	$3.29 \times 10^5 \pm 2.33 \times 10^4$	$2.79 \times 10^5 \pm 6.10 \times 10^4$
NaOH			
Potassium superoxide (mg)	Emission Intensity (RLU)	Emission Area (RLU)	Initial Velocities (RLU/s)
5	$7.67 \times 10^2 \pm 2.72 \times 10^1$	$1.21 \times 10^5 \pm 5.27 \times 10^3$	$1.19 \times 10^3 \pm 2.39 \times 10^2$
10	$7.90 \times 10^2 \pm 1.60 \times 10^1$	$1.27 \times 10^5 \pm 2.93 \times 10^3$	$1.47 \times 10^3 \pm 4.06 \times 10^2$
15	$6.38 \times 10^2 \pm 3.75 \times 10^1$	$7.66 \times 10^4 \pm 6.31 \times 10^3$	$1.67 \times 10^3 \pm 1.51 \times 10^2$

that of natural Coelenterazine (Chart 1). The chemiluminescence of Coelenterazine was also measured in aqueous solution with increasing amounts of superoxide anion. Measurements were performed at different pH values, by addition of either sodium acetate buffer pH 5.2 (1%), phosphate buffer pH 7.4 (75 mM), or NaOH (0.1 M). The representative chemiluminescence kinetic profiles at different pH in aqueous solution (in the presence of 10 mg) can be found in Fig. 3. We can already see some relevant differences regarding FBr-Cla (Fig. 2). Namely, while the profiles at acidic and basic pHs are similar between molecules, for natural Coelenterazine the profile at neutral pH is not identical to that obtained at acidic pH. Instead, that profile is somewhat a mixture between the profiles found at acidic and basic pH, as it does not present a sharp flash profile (as in acidic pH) but its decay is not so slow as found at basic pH. These results could indicate that the pKa of natural Coelenterazine is lower than that of FBr-Cla, meaning that its deprotonation starts to occur at neutral pH.

To verify if natural Coelenterazine presents the same relative response toward superoxide anion as toward FBr-Cla (decreasing emission with increasing superoxide anion), we plotted the light-emission intensity maxima of these imidazopyrazinones as a function of superoxide anion (Fig. 4), in aqueous solution in the presence of sodium acetate buffer pH 5.20 (1%). The light-emission intensities were presented as ratios, with the intensities obtained for each compound in the presence of 5 mg of superoxide anion used as reference. Interestingly, while both imidazopyrazinones possess dose-dependent responses, these are the opposite of each other. Namely, the light-emission intensity of Coelenterazine increases with increasing amounts of superoxide anion, while that of FBr-Cla decreases. These results once again point to FBr-Cla being sensitive to over-oxidation by superoxide anion.

A quantitative comparison between the light-emission efficiencies of

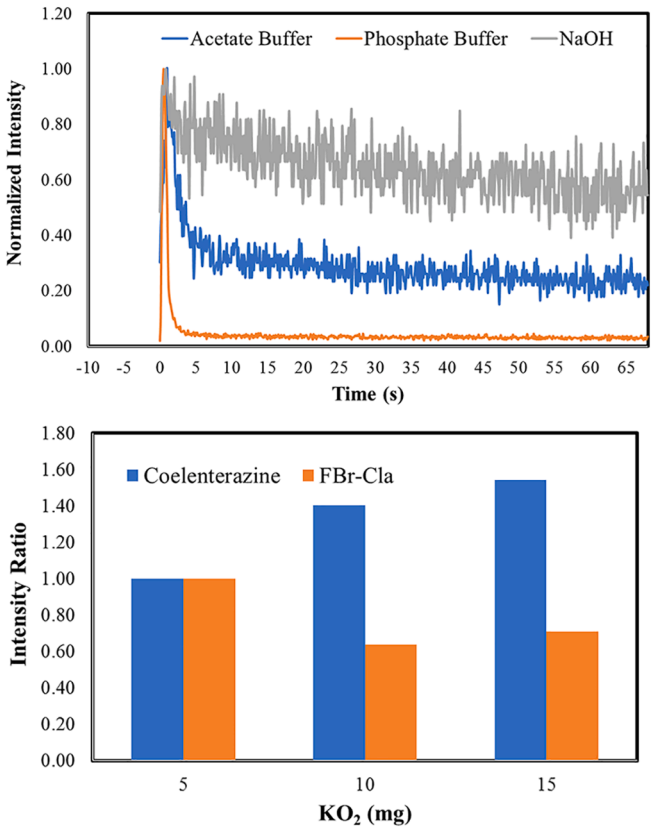

Fig. 4. Normalized chemiluminescence kinetic profile (top) for Coelenterazine in aqueous solution with addition of either sodium acetate buffer pH 5.2 (1%), phosphate buffer pH 7.4 (75 mM), or NaOH (0.1 M), in the presence of 10 mg of potassium superoxide. Chemiluminescence intensity ratios (bottom) for the reactions of both FBr-Cla and Coelenterazine in aqueous solution with addition of sodium acetate buffer pH 5.2 (1%), in the presence of increasing amounts of potassium superoxide (5 to 15 mg). The chemiluminescence intensities for each molecule in the presence of 5 mg of potassium superoxide were used as reference for both molecules. All assays depicted here performed for a final volume of 500 μL and a concentration of 5 μM for Coelenterazine and FBr-Cla.

FBr-Cla and Coelenterazine was performed by calculating the ratios ($\frac{FBr-Cla}{Coelenterazine}$) for the light-emission maxima intensities found in aqueous solution (Table 3). Interestingly, we obtained quite relevant ratios (from 3.61×10^0 to 2.70×10^3) in all pH values, which demonstrate that the superoxide anion-triggered chemiluminescence of FBr-Cla in aqueous solution is significantly enhanced in comparison with natural Coelenterazine. It should be noted that chemiluminescence reactions tend to present lower light-emitting intensities in aqueous solution due to energy loss to water molecules [49,50], with Coelenterazine not being an exception [14].

These very high ratios indicate that the structural modifications we made on the imidazopyrazinone core of Coelenterazine allow us to overcome this problem, thereby allowing for enhanced emission in aqueous solution, which could be very useful for superoxide anion-related sensing and imaging in biological media. In fact, besides being overexpressed in cancer cells, the unbalance of superoxide anion can also lead to deleterious health conditions such as inflammation and chronic granulomatous disease [51,52]. Superoxide anion is also involved in intra- and intercellular signalling pathways [53]. Thus, the sensitive and dynamic sensing of superoxide anion is required, with natural Coelenterazine already being validated as a suitable chemiluminescent probe [15,25,26]. Thus, the very enhanced emission of FBr-Cla indicates that this type of compound could serve as a basis for improving chemiluminescent probes in biological media. It should be noted that these results are similar to those found for a derivative of FBr-

Table 3
Measured ratios between the obtained light-emission intensity maxima (in RLU) for the chemiluminescence reactions of FBr-Cla and Coelenterazine ($\frac{FBr-Cla}{Coelenterazine}$) in aqueous solution with the addition of either sodium acetate buffer pH 5.2 (1%), phosphate buffer pH 7.4 (75 mM), or NaOH (0.1 M). Assays were performed for a final volume of 500 μL and a concentration of 5 μM for both imidazopyrazinones, as well as different amounts of potassium superoxide (5–15 mg).

Acetate Buffer	
Potassium superoxide (mg)	Emission Intensity (RLU)
5	$2.70 \times 10^3 \pm 5.45 \times 10^2$
10	$1.23 \times 10^3 \pm 1.61 \times 10^2$
15	$1.25 \times 10^3 \pm 1.79 \times 10^2$

Phosphate Buffer	
Potassium superoxide (mg)	Emission Intensity (RLU)
5	$2.12 \times 10^2 \pm 2.67 \times 10^1$
10	$3.21 \times 10^1 \pm 5.34 \times 10^0$
15	$3.51 \times 10^1 \pm 8.20 \times 10^0$

NaOH	
Potassium superoxide (mg)	Emission Intensity (RLU)
5	$3.61 \times 10^0 \pm 7.65 \times 10^{-1}$
10	$4.47 \times 10^0 \pm 6.63 \times 10^{-1}$
15	$4.37 \times 10^0 \pm 7.15 \times 10^{-1}$

Cla, with the only difference being the replacement of the fluorine heteroatom with a methoxy group [12]. These results indicate that the reason for this enhanced emission in aqueous solution could be related to the presence of an EWG group in the phenyl moiety and/or a bromine heteroatom directly attached to the imidazopyrazinone core [12]. Further investigation in this matter should be pursued in the future.

3.3. *In vitro evaluation of the cytotoxicity of FBr-Cla*

Having demonstrated that FBr-Cla is capable of being triggered by superoxide anion, an overexpressed cancer marker [25], our next step was then to evaluate its cytotoxicity toward different cancer cell lines: breast and prostate. As indicated before, FBr-Cla was designed as a hybrid between two different Cla compounds (Chart 2), which previously showed activity toward these cancer cell lines [36,37]. Compared with OHBr-Cla, the main difference is the presence of an EWG group instead of an EDG one in the phenyl moiety (Chart 2). Compared with Br-Cla, the main difference is the inclusion of a non-heavy-atom as EWG in the phenyl moiety and the presence of a heavy atom directly attached to the imidazopyrazinone core (Chart 2).

The first step of this evaluation was first to assess the safety and compatibility of FBr-Cla with non-cancer cells. Namely, lung fibroblast MCR-5 cell lines. The cytotoxicity of FBr-Cla toward these cells was measured with the standard MTT assay for exposure times of 48 h and a large concentration range of 1 to 100 μM (Fig. 5). Changes in cell morphology were observed by microscopy (Figure S7). Interestingly, FBr-Cla did not induce any toxicity toward MCR-5 (supported by analysis of cell morphology), which shows that this compound is compatible with non-cancer cells.

A similar analysis was also performed for both breast cancer MCF-7 (Fig. 5 **and** S8) and prostate cancer PC-3 (Fig. 5 **and** S9) cell lines. For breast cancer, FBr-Cla did only induce slight toxicity at the higher concentration of 100 μM. For prostate cancer, FBr-Cla was essentially inactive. Thus, these results indicate that FBr-Cla should be considered as not possessing anticancer activity, contrary to other brominated Cla compounds developed by members of this team [36–38]. Nevertheless, and despite being negative, these results provide much-needed structural insight into the anticancer activity of brominated Cla compounds.

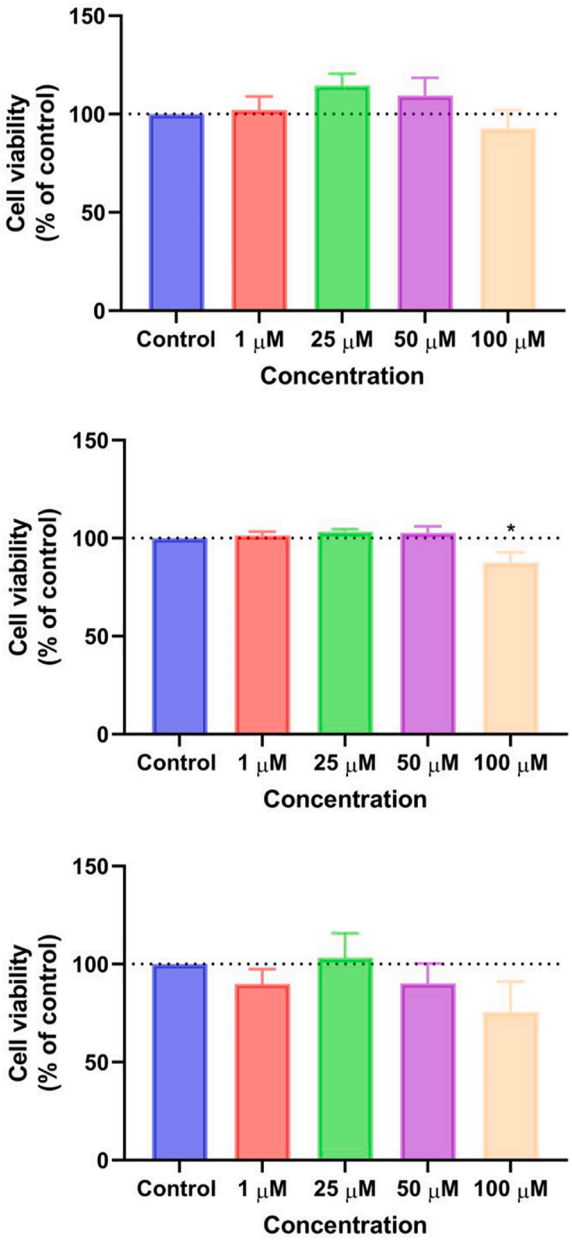

Fig. 5. Effect of FBr-Cla on the cellular viability of non-cancer lung fibroblast MCR-5 (top), breast cancer MCF-7 (middle), and prostate cancer PC-3 (bottom) cell lines. Cells were treated with vehicle (methanol) and increasing concentrations (0–100 μM) of FBr-Cla for 48 h and cell viability was assessed by the MTT assay. Data is given as the mean ± SEM (n = 3). * Statistically significant vs control (vehicle) at $p < 0.05$.

For instance, the absence of activity of FBr-Cla in comparison with Br-Cla (Chart 2), which presented IC_{50} values of ~22–24 μM for these cell lines [38], shows that the presence of bromine heteroatoms is not enough by itself for inducing anticancer properties to these compounds [36–38]. When comparing FBr-Cla (no activity) with that of OHBr-Cla (IC_{50} of 3.95 μM for prostate cancer) [36], it is possible to see that changing an EDG for an EWG group in the phenyl moiety is enough to eliminate all anticancer activity. Thus, OHBr-Cla-based compounds appear to possess a relevant sensitivity to small structural modifications. These insights should be useful for the future development of novel Cla-based compounds with anticancer activity. Especially if it is found why changing an EDG for an EWG group in the phenyl moiety of Cla compounds has a so relevant effect on the anticancer activity.

It should be noted that the anticancer activity of OHBr-Cla and Br-Cla

(Chart 2) [36–38], among others, was attributed to the enhanced generation of triplet states during their chemiluminescent reactions [36–38], which should then sensitize the highly cytotoxic singlet oxygen by energy transfer with molecular oxygen. By its turn, the enhanced generation of triplet states was to be achieved by the heavy-atom effect, due to the inclusion of bromine heteroatoms [33]. However, as shown in Table 3, the light-emission intensity maxima of FBr-Cla in aqueous solution is significantly enhanced. This points to this chemiluminescent reaction producing low triplet-to-singlet product ratios, as triplet states are easily quenched in solution. Thus, these data point to the absence of anticancer activity of FBr-Cla being the result of this compound being unable to generate triplet states (in appreciable yields) during its chemiluminescent reaction, despite the inclusion of bromine heteroatoms.

It should also be stated that these *in vitro* assays demonstrate the compatibility of FBr-Cla toward both non-cancer and cancer cells, especially at lower concentrations, which is beneficial for future uses of this type of molecule as a sensitive and dynamic probe for superoxide anion in biological media (as supported by its enhanced emission in aqueous solution).

Finally, one of the most promising strategies for increasing the efficiency of anticancer drugs is combination therapy, in which more than one molecule or modality is used to treat a single disease [54,55]. The combination of molecules/modalities can present relevant advantages, such as requiring lower dosages for achieving an equal or even high level of efficiency, which can be quite important to reduce the side effects of therapy [56]. Given this, we have also evaluated how increasing concentrations of FBr-Cla could affect the anticancer activity of the known chemotherapeutic agent 5-fluorouracil (5-FU). More specifically, we evaluated the cellular viability of both breast and prostate cancer cell lines in the presence of increasing concentrations of FBr-Cla and at the IC_{50} concentration of 5-FU (11.76 μM). Cellular viability was assessed with the standard MTT assay for an exposure period of 48 h. Results are presented in Fig. 6. Analysis of changes in cell morphology was found in **Figures S10 and S11**.

Increasing the concentration of FBr-Cla does not lead to great variations in the cellular viability of either cancer cell line (Fig. 6), as expected given the lack of anticancer activity of this compound. In fact, the decrease in cell viability that is indeed observed could be attributed to 5-FU. However, it can be seen that combining FBr-Cla with 5-FU does lead to some minor improvement in the profile of the chemotherapeutic agent (Fig. 6). This means that adding FBr-Cla could decrease the dosage of 5-FU required for a given effect. This is an interesting result, given the compatibility of FBr-Cla for non-cancer cells (Fig. 5). Thus, while FBr-Cla does not present relevant anticancer activity by itself, its use in a combination approach does lead to some improvement in the profile of a known chemotherapeutic agent.

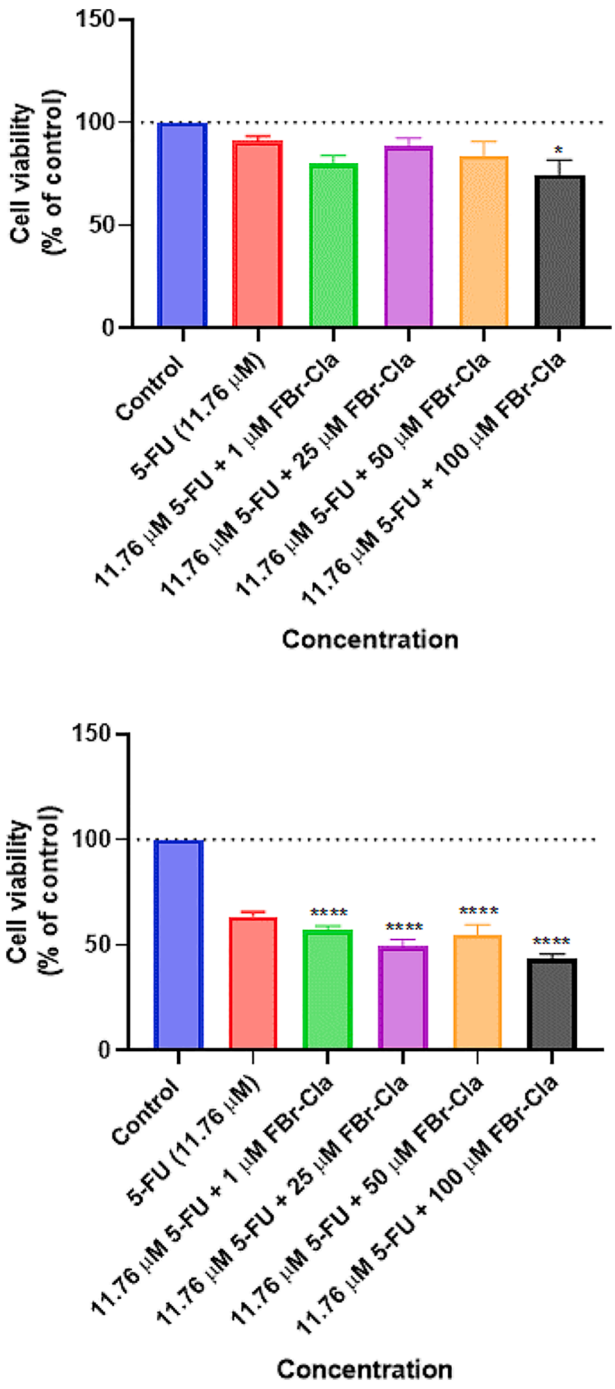

Fig. 6. Effect of combining FBr-Cla (1 to 100 μM) and 5-FU (11.76 μM) on the cellular viability of breast MCF-7 (top) and prostate PC-3 (bottom) cancer cell lines. Cells were treated with vehicle (methanol and DMSO) and increasing concentrations (0–100 μM) of FBr-Cla for 48 h and cell viability was assessed by the MTT assay. Data is given as the mean ± SEM (n = 3). * Statistically significant vs control (vehicle) at $p < 0.05$. **** Statistically significant vs control (vehicle) at $p < 0.0001$.

4. Conclusion

Here, we have described the synthesis and characterization of a new Coelenterazine brominated analog, FBr-Cla, which consisted of the imidazopyrazinone core functionalized with a fluorophenyl moiety, a bromine heteroatom, and a methyl group. This compound was found to be capable of pH-sensitive chemiluminescence, both in aprotic and protic (when triggered by superoxide anion) solvents. Relevantly, FBr-Cla was shown to possess a rather enhanced superoxide anion-induced chemiluminescence in aqueous solution, when in comparison with natural Coelenterazine.

Evaluation of the *in vitro* cytotoxicity of FBr toward both non-cancer (lung fibroblasts) and cancer (breast and prostate cells) revealed that this compound does not possess by itself relevant anticancer activity. In fact, it is compatible with both cancer and non-cancer cells. This analysis demonstrated that the addition of bromine heteroatom is not enough to introduce anticancer activity to this class of Coelenterazine derivatives. Furthermore, our results also showed that changing an electron-donating group by an electron-withdrawing one in the phenyl moiety is enough to eliminate all anticancer activity previously observed. Interestingly, while FBr-Cla has no appreciable anticancer activity, its use in a combination approach was able to improve the profile of a known chemotherapeutic agent.

In summary, in this study we reported a novel Coelenterazine analog with enhanced emission in aqueous solution when triggered by superoxide anion, and which is compatible with both non-cancer and cancer

cells. This compound has the potential to be used in the future as the basis for sensitive and dynamic chemiluminescent probes for superoxide anion in biological media. Moreover, we reported findings that allowed us to obtain relevant structural insight into the anticancer activity of brominated Coelenterazine analogs, which were found before to be capable of selective anticancer activity. This information should be useful to guide future optimizations of this system.

CRediT authorship contribution statement

José Pedro Silva: Investigation, Visualization, Writing – original draft. **Patricia González-Berdullas:** Visualization, Investigation, Writing – original draft. **Mariana Pereira:** Writing – original draft, Visualization, Investigation. **Diana Duarte:** Writing – review & editing, Investigation. **José E. Rodríguez-Borges:** Writing – review & editing. **Nuno Vale:** Writing – review & editing, Supervision, Funding acquisition. **Joaquim C.G. Esteves da Silva:** Writing – review & editing, Supervision, Funding acquisition. **Luís Pinto da Silva:** Supervision, Funding acquisition, Conceptualization, Writing – review & editing.

Declaration of Competing Interest

The authors declare that they have no known competing financial interests or personal relationships that could have appeared to influence the work reported in this paper.

Data availability

Data will be made available on request.

Acknowledgments

The Portuguese “Fundação para a Ciência e Tecnologia” (FCT, Lisbon) is acknowledged for funding of project PTDC/QUI-QFI/2870/2020, R&D Units CIQUP (UIDB/00081/2020), GreenUPorto (UIDB/05748/2020) and LAQV/REQUIMTE (UIDB/50006/2020), and Associated Laboratory IMS (LA/P/0056/2020). Luís Pinto da Silva acknowledges funding from FCT under the Scientific Employment Stimulus (2021.00768.CEECIND). Patricia González-Berdullas acknowledges funding for her postdoctoral position in the framework of project PTDC/QUI-QFI/2870/2020). The Laboratory of Computational Modelling of Environmental Pollutant-Human Interactions (LACOMEPHI) and the Materials Center of the University of Porto (CEMUP) are acknowledged. Diana Duarte acknowledges FCT for funding her PhD grant (SFRH/143211/2019). Mariana Pereira acknowledges FCT for funding her PhD grant (2021.07450.BD). Nuno Vale acknowledges funding from FEDER—Fundo Europeu de Desenvolvimento Regional through the COMPETE 2020—Operational Programme for Competitiveness and Internationalization (POCI), Portugal 2020, and by FCT, in a framework of the projects in CINTESIS, R&D Unit (reference UIDB/4255/2020) and within the scope of the project “RISE - LA/P/0053/2020. Nuno Vale also thanks support from FCT and FEDER (European Union), award number IF/00092/2014/CP1255/CT0004 and CHAIR in Onco-Innovation at FMUP.

Appendix A. Supplementary data

Supplementary data to this article can be found online at https://doi.org/10.1016/j.jphotochem.2022.114228.

References

[1] L. Pinto da Silva, J.C.G. Esteves da Silva, Firefly Chemiluminescence and Bioluminescence: Efficient Generation of Excited States, ChemPhysChem 13 (2012) 2257–2262.
[2] M. Vacher, I. Fdez, B.-W. Galván, S. Ding, R. Schramm, P. Berraud-Pache, N. Naumov, Y.-J. Ferré, I. Liu, D. Navizet, W.J. Roca-Sanjuán, R.L. Baader, Chemi- and bioluminescence of cyclic peroxides, Chem. Rev. 118 (2018) 6927–6974.
[3] F.A. Augusto, G.A. de Souza, S.P. de Souza Júnior, M. Khalid, W.J. Baader, Efficiency of electron transfer initiated chemiluminescence, Photochem. Photobiol. 89 (2013) 1299–1317.
[4] A. Boaro, R.A. Reis, C.S. Silva, D.U. Melo, A.G.G.C. Pinto, F.H. Bartoloni, Evidence for the formation of 1,2-dioxetane as a high-energy intermediate and possible chemiexcitation pathways in the chemiluminescence of lophine peroxides, J. Org. Chem. 86 (2021) 6633–6647.
[5] F.A. Augusto, F.H. Bartoloni, A.P.E. Pagano, W.J. Baader, Mechanistic study of the peroxyoxalate system in completely aqueous carbonate buffer, Photochem. Photobiol. 97 (2021) 309–316.
[6] A. Giussani, P. Farahani, D. Martínez-Muñoz, M. Lundberg, R. Lindh, D. Roca-Sanjuán, Molecular basis of the chemiluminescence mechanism of luminol, Chem. Eur. J. 25 (2019) 5202–5213.
[7] Z.M. Kaskova, A.S. Tsarkova, I.V. Yampolsky, 1001 Lights: luciferins, luciferases, their mechanisms of action and applications in chemical analysis, biology and medicine, Chem. Soc. Rev. 45 (2016) 6048–6077.
[8] C.-G. Min, P.J.O. Ferreira, L. Pinto da Silva, Theoretically obtained insight into the mechanism and dioxetanone species responsible for the singlet chemiexcitation of Coelenterazine, J. Photochem. Photobiol. B, Biol. 174 (2017) 18–26.
[9] T. Jiang, L. Du, M. Li, Lighting up bioluminescence with coelenterazine: strategies and applications, Photochem. Photobiol. Sci. 15 (2016) 466–480.
[10] S.H.D. Haddock, M.A. Moline, J.F. Case, Bioluminescence in the sea, Ann. Rev. Mar. Sci. 2 (2009) 443–493.
[11] C.M. Magalhães, J.C.G. Esteves da Silva, L. Pinto da Silva, Study of coelenterazine luminescence: Electrostatic interactions as the controlling factor for efficient chemiexcitation, J. Lumin. 199 (2018) 339–347.
[12] J.P. Silva, P. González-Berdullas, J.C.G. Esteves da Silva, L. Pinto da Silva, Development of a coelenterazine derivative with enhanced superoxide anion-triggered chemiluminescence in aqueous solution, Chemosensors 10 (2022).
[13] C.M. Magalhães, J.C.G. Esteves da Silva, L. Pinto da Silva, Comparative study of the chemiluminescence of coelenterazine, coelenterazine-e and Cypridina luciferin with an experimental and theoretical approach, J. Photochem. Photobiol. B: Biol. 190 (2019) 21–31.
[14] J.M. Lourenço, J.C.G. Esteves da Silva, L. Pinto da Silva, Combined experimental and theoretical study of Coelenterazine chemiluminescence in aqueous solution, J. Lumin. 194 (2018) 139–145.
[15] K. Teranishi, Non-invasive and accurate readout of superoxide anion in biological systems by near-infrared light, Anal. Chim. Acta 1179 (2021), 338827.
[16] G. Gagnot, V. Hervin, E.P. Coutant, S. Goyard, Y. Jacob, T. Rose, F.E. Hibti, A. Quatela, Y.L. Janin, Core-modified coelenterazine luciferin analogues: synthesis and chemiluminescence properties, Chem. Eur. J. 27 (2021) 2112–2123.
[17] V.V. Krasitskaya, E.E. Bashmakova, L.A. Frank, Coelenterazine-dependent luciferases as a powerful analytical tool for research and biomedical applications, Int. J. Mol. Sci. 21 (2020).
[18] R. Nishihara, M. Abe, S. Nishiyama, D. Citterio, K. Suzuki, S.B. Kim, Luciferase-specific coelenterazine analogues for optical contamination-free bioassays, Sci. Rep. 7 (2017) 908.
[19] L.P. Burakova, M.S. Lyakhovich, K.S. Mineev, V.N. Petushkov, R.I. Zagitova, A. S. Tsarkova, S.I. Kovalchuk, I.V. Yampolsky, E.S. Vysotski, Z.M. Kaskova, Unexpected coelenterazine degradation products of beroe abyssicola photoprotein photoinactivation, Org. Lett. 23 (2021) 6846–6849.
[20] E.V. Eremeeva, T. Jiang, N.P. Malikova, M. Li, E.S. Vysotski, Bioluminescent properties of semi-synthetic obelin and aequorin activated by coelenterazine analogues with modifications of C-2, C-6, and C-8 substituents, Int. J. Mol. Sci. 21 (2020).
[21] S. Gnaim, D. Shabat, Self-immolative chemiluminescence polymers: innate assimilation of chemiexcitation in a domino-like depolymerization, J. Am. Chem. Soc. 139 (2017) 10002–10008.
[22] T. Mikroulis, M.C. Cuquerella, A. Giussani, A. Pantelia, G.M. Rodríguez-Muñiz, G. Rotas, D. Roca-Sanjuán, M.A. Miranda, G.C. Vougioukalakis, Building a functionalizable, potent chemiluminescent agent: a rational design study on 6,8-substituted luminol derivatives, J. Org. Chem. 86 (2021) 11388–11398.
[23] S.M. Marques, F. Peralta, J.C.G. Esteves da Silva, Optimized chromatographic and bioluminescent methods for inorganic pyrophosphate based on its conversion to ATP by firefly luciferase, Talanta 77 (2009) 1497–1503.
[24] K.K. Krzymiński, A.D. Roshal, P.B. Rudnicki-Velasquez, K. Żamojć, On the use of acridinium indicators for the chemiluminescent determination of the total antioxidant capacity of dietary supplements, Luminescence 34 (2019) 512–519.
[25] L.L. Bronsart, C. Stokes, C.H. Contag, Multimodality imaging of cancer superoxide anion using the small molecule coelenterazine, Mol. Imaging Biol. 18 (2016) 166–171.
[26] L.L. Bronsart, C. Stokes, C.H. Contag, Chemiluminescence imaging of superoxide anion detects beta-cell function and mass, PloS one 11 (2016) e0146601–e.
[27] M. Yang, J. Huang, J. Fan, J. Du, K. Pu, X. Peng, Chemiluminescence for bioimaging and therapeutics: recent advances and challenges, Chem. Soc. Rev. 49 (2020) 6800–6815.
[28] M. Cronin, A.R. Akin, K.P. Francis, M. Tangney, In vivo bioluminescence imaging of intratumoral bacteria, in: R. Hoffman (Ed.), Bacterial Therapy of Cancer. Methods in Molecular Biology, Humana Press, New York, NY, 2016.
[29] K.M. Grinstead, L. Rowe, C.M. Ensor, S. Joel, P. Daftarian, E. Dikici, J.-M. Zingg, S. Daunert, Red-shifted aequorin variants incorporating non-canonical amino acids: applications in in vivo imaging, PloS One 11 (2016) e0158579–e.

[30] N. Gaspar, J.R. Walker, G. Zambito, K. Marella-Panth, C. Lowik, T.A. Kirkland, L. Mezzanotte, Evaluation of NanoLuc substrates for bioluminescence imaging of transferred cells in mice, J. Photochem. Photobiol. B 216 (2021), 112128.
[31] Y. Li, C. Wang, L. Zhou, S. Wei, A 2-pyridone modified zinc phthalocyanine with three-in-one multiple functions for photodynamic therapy, Chem. Comm. 57 (2021) 3127–3130.
[32] X. Li, Z. Shi, J. Wu, J. Wu, C. He, X. Hao, C. Duan, Lighting up metallohelices: from DNA binders to chemotherapy and photodynamic therapy, Chem. Comm. 56 (2020) 7537–7548.
[33] Y.-F. Xiao, J.-X. Chen, W.-C. Chen, X. Zheng, C. Cao, J. Tan, X. Cui, Z. Yuan, S. Ji, G. Lu, W. Liu, P. Wang, S. Li, C.-S. Lee, Achieving high singlet-oxygen generation by applying the heavy-atom effect to thermally activated delayed fluorescent materials, Chem. Comm. 57 (2021) 4902–4905.
[34] W. Fan, P. Huang, X. Chen, Overcoming the Achilles' heel of photodynamic therapy, Chem. Soc. Rev. 45 (2016) 6488–6519.
[35] S. Yano, S. Hirohara, M. Obata, Y. Hagiya, S.-I. Ogura, A. Ikeda, H. Kataoka, M. Tanaka, T. Joh, Current states and future views in photodynamic therapy, J. Photochem. Photobiol. C: Photochem. Rev. 12 (2011) 46–67.
[36] L. Pinto da Silva, C.M. Magalhães, A. Núñez-Montenegro, P.J.O. Ferreira, D. Duarte, J.E. Rodríguez-Borges, N. Vale, J.C.G. Esteves da Silva, Study of the combination of self-activating photodynamic therapy and chemotherapy for cancer treatment, Biomolecules 9 (2019).
[37] L. Pinto da Silva, A. Núñez-Montenegro, C.M. Magalhães, P.J.O. Ferreira, D. Duarte, P. González-Berdullas, J.E. Rodríguez-Borges, N. Vale, J.C.G. Esteves da Silva, Single-molecule chemiluminescent photosensitizer for a self-activating and tumor-selective photodynamic therapy of cancer, Eur. J. Med. Chem. 183 (2019), 111683.
[38] C.M. Magalhães, P. González-Berdullas, D. Duarte, A.S. Correia, J.E. Rodríguez-Borges, N. Vale, J.C.G. Esteves da Silva, L. Pinto da Silva, Target-oriented synthesis of marine coelenterazine derivatives with anticancer activity by applying the heavy-atom effect, Biomedicines 9 (2021).
[39] C.M. Magalhães, J.C.G. Esteves da Silva, L. Pinto da Silva, Chemiluminescence and bioluminescence as an excitation source in the photodynamic therapy of cancer: a critical review, ChemPhysChem 17 (2016) 2286–2294.
[40] L. Pinto da Silva, C.M. Magalhães, D.M.A. Crista, J.C.G. Esteves da Silva, Theoretical modulation of singlet/triplet chemiexcitation of chemiluminescent imidazopyrazinone dioxetanone via C8-substitution, Photochem. Photobiol. Sci. 16 (2017) 897–907.
[41] T. Hirano, Y. Takahashi, H. Kondo, S. Maki, S. Kojima, H. Ikeda, H. Niwa, The reaction mechanism for the high quantum yield of Cypridina (Vargula) bioluminescence supported by the chemiluminescence of 6-aryl-2-methylimidazo [1,2-a]pyrazin-3(7H)-ones (Cypridina luciferin analogues), Photochem. Photobiol. Sci. 7 (2008) 197–207.
[42] R. Saito, T. Hirano, S. Maki, H. Niwa, Synthesis and chemiluminescent properties of 6,8-diaryl-2-methylimidazo[1,2-a]pyrazin-3(7H)-ones: Systematic investigation of substituent effect at para-position of phenyl group at 8-position, J. Photochem. Photobiol. A: Chem. 293 (2014) 12–25.
[43] T. Hirano, Y. Gomi, T. Takahashi, K. Kitahara, C. Feng Qi, I. Mizoguchi, S. Kyushin, M. Ohashi, Chemiluminescence of coelenterazine analogues - Structures of emitting species, Tetrahedron Lett. 33 (1992) 5771–5774.
[44] L. Pinto da Silva, R.F.J. Pereira, C.M. Magalhães, J.C.G. Esteves da Silva, Mechanistic insight into cypridina bioluminescence with a combined experimental and theoretical chemiluminescent approach, J. Phys. Chem. B 121 (2017) 7862–7871.
[45] L. Pinto da Silva, J.C.G. Esteves da Silva, Kinetics of inhibition of firefly luciferase by dehydroluciferyl-coenzyme A, dehydroluciferin and l-luciferin, Photochem. Photobiol. Sci. 10 (2011) 1039–1045.
[46] C. Ribeiro, J.C.G. Esteves da Silva, Kinetics of inhibition of firefly luciferase by oxyluciferin and dehydroluciferyl-adenylate, Photochem. Photobiol. Sci. 7 (2008) 1085–1090.
[47] M. Hayyan, M.A. Hashim, I.M. AlNashef, Superoxide ion: generation and chemical implications, Chem. Rev. 116 (2016) 3029–3085.
[48] D.T. Sawyer, J.S. Valentine, How super is superoxide? Acc. Chem. Res. 14 (1981) 393–400.
[49] S. Gnaim, O. Green, D. Shabat, The emergence of aqueous chemiluminescence: new promising class of phenoxy 1,2-dioxetane luminophores, ChemComm 54 (2018) 2073–2085.
[50] O. Green, T. Eilon, N. Hananya, S. Gutkin, C.R. Bauer, D. Shabat, Opening a gateway for chemiluminescence cell imaging: distinctive methodology for design of bright chemiluminescent dioxetane probes, ACS Cent. Sci. 3 (2017) 349–358.
[51] G. Waris, H. Ahsan, Reactive oxygen species: Role in the development of cancer and various chronic conditions, J. Carcinog. 5 (2006) 14.
[52] D.E. Arnold, J.R. Heimall, A review of chronic granulomatous disease, Adv. Ther. 34 (2017) 2543–2557.
[53] B.C. Dickinson, C.J. Chang, Chemistry and biology of reactive oxygen species in signaling or stress responses, Nat. Chem. Biol. 7 (2011) 504–511.
[54] S. Silva, A.J. Almeida, N. Vale, Combination of cell-penetrating peptides with nanoparticles for therapeutic application: a review, Biomolecules 9 (2019) 22.
[55] A. Correia, D. Silva, A. Correia, M. Vilanova, F. Gärtner, N. Vale, Study of new therapeutic strategies to combat breast cancer using drug combinations, Biomolecules 8 (2018).
[56] K. Han, E.E. Jeng, G.T. Hess, D.W. Morgens, A. Li, M.C. Bassik, Synergistic drug combinations for cancer identified in a CRISPR screen for pairwise genetic interactions, Nat. Biotechnol. 35 (2017) 463–474.